

Coagulation and Fragmentation: Universal Steady-State Particle-Size Distribution

Patrick T. Spicer and Sotiris E. Pratsinis

Dept. of Chemical Engineering, University of Cincinnati, Cincinnati, OH 45221

A population balance model presented describes simultaneous coagulation and fragmentation during shear-induced flocculation. Given sufficient time, a floc-size distribution reaches steady state that reflects the balance between coagulation and fragmentation. The model agrees with experimental data for the evolution of the average floc size. Higher shear shifts the steady-state size distribution to smaller sizes. When the steady-state size distributions obtained at various shear rates are scaled with the average floc size, however, they collapse onto a single line. This indicates that the steady-state floc-size distribution is self-preserving with respect to fluid shear. This distribution is universal for the employed coagulation and fragmentation rates provided that less than 5% (by number) of the particles remain unflocculated. This result is supported with experimental data on shear-induced flocculation of polystyrene particles, although a detailed quantitative comparison is limited by the irregular structure of the flocs.

Introduction

Simultaneous coagulation and fragmentation by fluid shear is encountered in processes involving polymerization (Blatz and Tobolsky, 1945; Alvarez et al., 1994), liquid-liquid dispersion (Coulaloglou and Tavlarides, 1977), emulsification (Danov et al., 1994), and flocculation (Lu and Spielman, 1985). The removal of fine particles from drinking or wastewater (Tambo, 1991) and the recovery of particulate products/microbial biomass from bioreactors (Shamlou and Tichener-Hooker, 1993) is often facilitated by enlarging their size by flocculation.

Most flocculators are operated under shear (Parker et al., 1972) assuring thorough mixing and high collision frequency between particles and therefore rapid particle (floc) growth. During shear-induced flocculation, a flocculant is added to the suspension to destabilize it. Early on, the particles rapidly grow by shear-driven coagulation. As the particles become larger, however, they become vulnerable to breakage by fluid-particle interactions. After some time, a steady state is reached between floc growth and breakage as the floc-size distribution no longer changes with time (Reich and Vold, 1959). Liquid-liquid dispersions exhibit similar behavior, as an asymptotic droplet-size distribution is attained by the balance between droplet coalescence and breakage (Delichatsios and Probstein, 1976).

A common approach to describe the dynamics of this process has been to combine the collision frequency for shear-induced coagulation (Saffman and Turner, 1956) with various descriptions of particle breakage in the framework of the population balance equation. This approach has been used primarily to describe or fit experimental data (Boadway, 1978; Grabenbauer and Glatz, 1981; Lu and Spielman, 1985; Burban et al., 1989; Peng and Williams, 1994). More detailed fluid mechanics-based stochastic models account for the effect of fluid shear field variations on flocculation kinetics (Kim and Glasgow, 1987).

Vigil and Ziff (1989) studied numerically the existence of a steady-state size distribution for various forms of coagulation and fragmentation rates using moment solutions to the population balance equation. A combination of these rates was termed stable if a steady-state solution exists. For a particle volume-dependent coagulation rate (as in the case of shear coagulation) a steady-state size distribution exists for a positive power dependence of the breakage rate on particle volume. Tambo and Watanabe (1979) used a population balance model to describe the steady-state floc size distributions attained during flocculation and sedimentation of kaolin suspensions. Their model incorporated a simplified description of breakage and predicted a steady-state floc-size distribution that was self-preserving with respect to maximum floc size when scaled by an arbitrary factor. When the steady-state size

Correspondence concerning this article should be addressed to S. E. Pratsinis.

distributions (scaled by the average particle volume) collapse onto a single-size distribution, this distribution is termed self-preserving (Friedlander and Wang, 1966). Family et al. (1986) found good agreement between the descriptions of a coagulation-fragmentation process given by a population balance model and by one-, two-, and three-dimensional Monte Carlo simulations. They also observed that the steady-state cluster size distribution was self-preserving when scaled by the fragmentation rate constant. Cohen (1990) developed a combinatoric model of the steady-state floc-size distribution assuming growth and breakage. This model predicted a steady-state floc-size distribution that was self-preserving with respect to initial number concentration (Cohen, 1992). Comparisons with experimental results indicated that the model was better suited to describe coalescence and breakage in a liquid-liquid dispersion.

The main objective of this work is to examine the self-similarity of the steady-state floc size distribution (SSFSD) and to study the effect of shear rate and the fragment-size distribution on the shape of the SSFSD. Previous work has shown theoretically the existence of the self-preserving distribution, but only for simplified models: Tambo and Watanabe (1979) assumed that flocs broke reversibly (which is a very special case), the model of Family et al. (1986) used generalized descriptions of coagulation and fragmentation, and Cohen (1992) considered only the most probable collisions in his model. In addition, these studies did not provide experimental support of the theoretical results. Tambo and Watanabe (1979) showed a settling time distribution that was self-preserving only when normalized twice by arbitrary parameters. The model used in this work accounts for all possible collisions and has been used previously to describe realistic systems (Lu and Spielman, 1985). Furthermore, the model is capable of describing the experimental evolution of the average floc size and the floc-size distribution to steady state.

The objective of this article is to present a model that describes particle coagulation and fragmentation concisely and describes the attainment of the steady-state floc-size distribution during shear-induced flocculation. The effect of process variables on this distribution is investigated. For a fixed collision frequency and fragmentation mode, steady-state size distributions obtained at various shear rates collapse onto a single-size distribution when normalized with the average floc size. This type of asymptotic behavior may be used to infer theoretical descriptions of floc growth and breakage kinetics (Wright and Ramkrishna, 1994). The predictions of the model are compared with experimental data for the flocculation of polystyrene with alum and NaCl.

Theory

During the initial stages of shear-induced flocculation, particle growth is dominant and the average particle (floc) size increases rapidly by shear-induced coagulation. As the flocs grow and become comparable to the size of fluid eddies, the significance of fragmentation (breakage) increases. Thus, the rate of change of the particle (floc) concentration by coagulation and fragmentation is given by (Austin, 1971; Friedlander, 1977)

$$\frac{dn_i}{dt} = \frac{l}{2} \sum_{j+k=i} \alpha\beta(u_j, u_k)n_j n_k - n_i \sum_{k=1}^{\max} \alpha\beta(u_k, u_i)n_k - S_i n_i + \sum_{j=i}^{\max} \gamma_{i,j} S_j n_j \quad (1)$$

where n_i is the number concentration of flocs of size i (meaning that a single floc contains i primary particles), α is the collision efficiency or the fraction of collisions that result in coagulation, and $\beta(u_i, u_k)$ is the collision frequency for particles of volume u_i and u_k . S_i is the fragmentation rate of flocs of size i , and $\gamma_{i,j}$ is the breakage distribution function defining the volume fraction of the fragments of size i coming from j -sized particles. Here, the index max represents the largest particle size that will form fragments of size i upon breakage. The first term on the righthand side of Eq. 1 represents the formation of particles comprised of i primary particles by collisions of smaller j - and k -sized particles. The second righthand-side term denotes the loss of particles of size i by collision with particles of any other size. The third righthand side term describes the loss of particles of size i by fragmentation and the fourth righthand side term describes the formation of particles of size i by the fragmentation of larger particles.

The coagulation-fragmentation process occurs over a wide size range so a discrete model of flocculation may require excessive computation time (Landgrebe and Pratsinis, 1990). The employed size domain is divided into ranges or sections to ease computation. Equations describing the particle number concentration within each section are used. Each section is represented by a characteristic volume V_i that is the average volume of the sizes contained in the section

$$V_i = \frac{b_{i-1} + b_i}{2} \quad (2)$$

where b_i is the upper boundary volume of section i (e.g., $b_i = u_i$). V_i is also a function, (sectional spacing) f , of the previous section V_{i-1}

$$V_i = fV_{i-1} \quad (3)$$

In this study, a numerical technique is used to simulate the evolution of the particle-size distribution with $f = 2$ (Hounslow et al., 1988; Kusters et al., 1993)

$$\begin{aligned} \frac{dN_i}{dt} = & \sum_{j=1}^{i-2} 2^{j-i+1} \alpha\beta_{i-1,j} N_{i-1} N_j + \frac{1}{2} \alpha\beta_{i-1,i-1} N_{i-1}^2 \\ & - N_i \sum_{j=1}^{i-1} 2^{j-i} \alpha\beta_{i,j} N_j \\ & - N_i \sum_{j=i}^{i \max} \alpha\beta_{i,j} N_j - S_i N_i + \sum_{j=i}^{i \max} \Gamma_{i,j} S_j N_j \quad (4) \end{aligned}$$

where $\Gamma_{i,j}$ is the breakage distribution function from Eq. 1 modified to conserve volume within the framework of the sectional model, and N_i is the number concentration of flocs

with volume V_i . Thus, the number of equations that needs to be solved is the same as the number of sections. Calculations were carried out using 30 sections, from $i = 1$ to i max

$$V_i = u_1 2^{i-1} \quad (5)$$

where u_1 is the primary particle volume; the model spans a size range of flocs composed of one to 2^{29} primary particles. The minimum size corresponds to the smallest particle size used in experiments (Oles, 1992; Spicer, 1995).

The collision frequency for turbulent shear-induced coagulation in the absence of viscous retardation and floc structural effects is (Saffman and Turner, 1956)

$$\beta(V_i, V_j) = 0.31G(V_i^{1/3} + V_j^{1/3})^3 \quad (6)$$

where G is the spatially averaged velocity gradient (Camp and Stein, 1943).

The fragmentation rate is given as a function of particle volume by (Kapur, 1972)

$$S_i = AV_i^a \quad (7)$$

where $a = 1/3$. This is consistent with the theoretical expectation that breakage rate is proportional to the floc diameter (Boadway, 1978; Peng and Williams, 1994) and A is the breakage rate coefficient for shear-induced fragmentation (Pandya and Spielman, 1982)

$$A = A'G^y \quad (8)$$

where y is a constant inversely proportional to the floc strength and A' is a proportionality constant that is determined experimentally.

The most common breakage mechanisms are: (a) erosion of primary particles or small fragments from the floc surface;

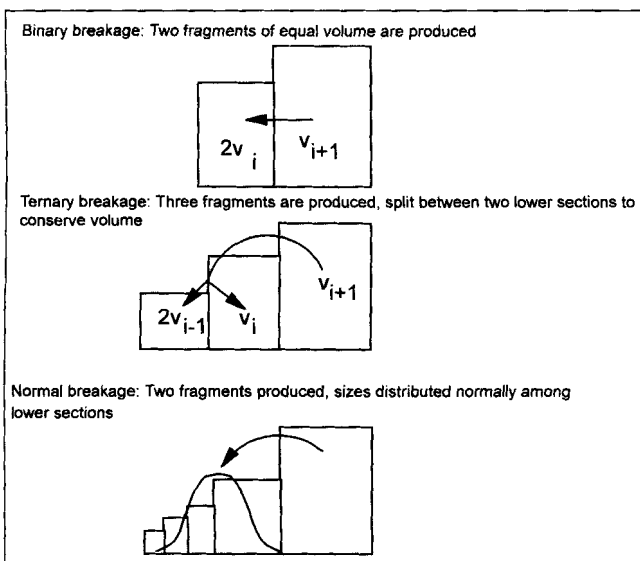


Figure 1. Three types of fragment-size distributions during shear-induced flocculation.

and (b) “bulgy deformation” rupture or splitting of the floc (Parker et al., 1972; Pandya and Spielman, 1982; Akers et al., 1987). Erosion results from fluid eddies comparable to the floc size. The splitting mechanism arises from pressure differences on the opposite sides of the floc that induce a shearing type of fragmentation (Parker et al., 1972).

Here, three distinct breakage distribution functions ($\Gamma_{i,j}$) were investigated (Figure 1) for the sectional description of coagulation and fragmentation:

$$a. \Gamma_{i,j} = \frac{V_j}{V_i}; \text{ binary breakage, so max} = i + 1 \text{ (Chen et al., 1990)}$$

$$b. \Gamma_{i,j} = \frac{V_j}{2V_i}; \text{ ternary breakage, so max} = i + 2$$

$$c. \Gamma_{i,j} = \frac{V_j}{V_i} \int_{b_{i-1}}^{b_i} \frac{1}{\sqrt{2\pi}\sigma_f} \exp\left[-\frac{(V - V_{fa})^2}{2\sigma_f^2}\right] dV;$$

normally distributed fragments, so max = maximum i (Coulaloglou and Tavlarides, 1977) (9)

where V_{fa} is the mean volume of the fragment-size distribution (which is half the volume of the fragmenting floc), and σ_f is the standard deviation of the fragment-size distribution (Coulaloglou and Tavlarides, 1977)

$$\sigma_f = \frac{V_j}{\lambda} \quad (10)$$

where V_j is the parent floc undergoing fragmentation and λ is a variable. The larger the value of λ , the narrower is the fragment-size distribution. Pandya and Spielman (1982) found that floc splitting produced 2–3 daughter fragments that were similar in size. They modeled floc splitting by assuming the floc fragments were distributed normally in size. The lower summation limit of $j = i$ in Eq. 4 accounts for any fragments that remain in the section after breakage of an i -sized particle. However, in the implementation of the binary and ternary fragment-size distributions the summation is carried out from a lower limit of $j = i + 1$. For the case of the normal fragment size distribution, the summation is carried out from a lower limit of $j = i$.

In order to conserve volume for the case of the normal fragment-size distribution, the volume fraction of particles in section i formed by fragmentation of a particle in section j is found by integrating $\Gamma_{i,j}$ (Eq. 9c) across sections 1 to j , summing these volume fractions, and then normalizing each $\Gamma_{i,j}$ value with this sum to ensure that it sums to one. The fragment size distribution expressions in Eq. 9 are only valid for the $f = 2$ discretization. The formulation in Eqs. 7–9 best describes fragmentation by splitting, assuming that the splitting mode of breakage is more significant than erosion. This assumption is justified later on. Equations 6–10 were substituted into Eq. 4 and the sectional model was solved numerically using DGEAR, an ordinary differential equation solver (IMSL, 1989).

Experimental Studies

Flocculation of monodisperse polystyrene particles (primary particle size, $d_1 = 0.87 \mu\text{m}$ by TEM) was investigated in a 2.8 L, baffled, stirred tank using a six bladed, disk mounted Rushton impeller. The impeller rotational velocity was measured with an Ono Sokki HT-4100 optical tachometer. The turbulent shear rate within the stirred tank was characterized using the spatially averaged velocity gradient G (Camp and Stein, 1943)

$$G = \left(\frac{\epsilon}{\nu} \right)^{1/2} \quad (11)$$

where ν is the kinematic viscosity of the suspending fluid (here, water) and ϵ is the average turbulent energy dissipation rate (Godfrey et al., 1989)

$$\epsilon = \left(\frac{P_o N^3 D^5}{V} \right) \quad (12)$$

where P_o is the impeller power number, N is the impeller speed, V is the stirred tank volume, and D is the impeller diameter. The P_o is obtained from the standard power curve for the employed six-blade impeller (Holland and Chapman, 1966). Although the flow conditions within a stirred tank are nonhomogeneous (Cutter, 1966; Sprow, 1967; Konno et al., 1983), Eqs. 11 and 12 are used to provide a basis for comparison with previous work.

The polystyrene particles were flocculated in distilled water at a solids volume fraction of $\phi = 8.3 \times 10^{-5}$, corresponding to an initial number concentration of $N_o = 2.4 \times 10^8 \text{ cm}^{-3}$. An acidic solution of aluminum sulfate hydrate or alum ($\text{Al}_2(\text{SO}_4)_3 \cdot 16\text{H}_2\text{O}$) (Aldrich, 98%) was added to promote flocculation. The suspension was buffered with sodium hydrogen carbonate (NaHCO_3) (Aldrich, 99%) at a concentration of 1 mM. The pH was kept neutral (7 ± 0.1) during all experiments. The polystyrene particles were suspended and then stirred at $G = 540 \text{ s}^{-1}$ for 5 min to break up any agglomerates. A measured amount of flocculant was then added and mixed with the suspension for 1 min at $G = 540 \text{ s}^{-1}$. Following this rapid mixing, flocculation was carried out at a constant G ranging from 63–129 s^{-1} and alum concentration, $c = 32 \text{ mg/L}$. Samples were withdrawn for floc-size analysis using a Nikon Labophot microscope (40X, 100X, 400X) connected to a Hitachi-Denshi CCTV camera. Image analysis was performed using Global Lab Image v. 2.0 software, and detailed floc-size distributions were counted by measuring the maximum length L of the individual flocs (Spicer and Pratsinis, 1996).

Results and Discussion

Dynamics of shear-induced flocculation

The sectional model was validated for pure coagulation of an initially exponential size distribution of particles with a size-dependent collision frequency that closely resembles the shear-induced collision frequency in Eq. 6. The predictions of the model were in excellent agreement with analytical solutions (Golovin, 1963; Hounslow et al., 1988). The model

predictions for pure fragmentation of an initially monodisperse suspension of spherical particles were also in excellent agreement with analytical solutions (Williams, 1990; Kusters et al., 1993). The predictions of the model for simultaneous coagulation and fragmentation also agreed well with the analytical solution for this case (Blatz and Tobolsky, 1945). During all calculations the loss of total volume ($\sum N_i V_i$) was monitored and found to be less than 1% indicating the robustness of this model to domain error.

Figure 2 shows an example calculation of the evolution of the floc number distribution for an initially monodisperse suspension undergoing shear-induced flocculation, assuming binary breakage of flocs for $\alpha = 1$, $G = 100 \text{ s}^{-1}$, $A = 1$, $N_1 = 9.3 \times 10^6 \text{ cm}^{-3}$, and $d_1 = 2.17 \mu\text{m}$ (Oles, 1992). The distribution quickly grows into larger sizes and 25% of the initial particles have been flocculated ($N_1/N_{\text{tot}} = 0.75$) after only one min. After 75 min, the primary particles are depleted further by coagulation while the larger ones begin to form a bell-shaped size distribution. Later on at 100 min, the distribution shifts to slightly larger sizes, and at 140 min it forms a bell-shaped curve that does not grow any larger. Fragmentation prevents further growth so the distribution changes very little with time and can be considered to be at steady state. For example, at 180 min the distribution is indistinguishable from that attained at 140 min. The above picture is typical of this process and has been well documented experimentally (Tambo and Watanabe, 1979; Kusters, 1991; Oles, 1992). This is also in agreement with the results of Vigil and Ziff (1989) predicting the attainment of steady state for the employed coagulation and fragmentation kernels.

Determination of model parameters

To compare the model predictions with experimental data,

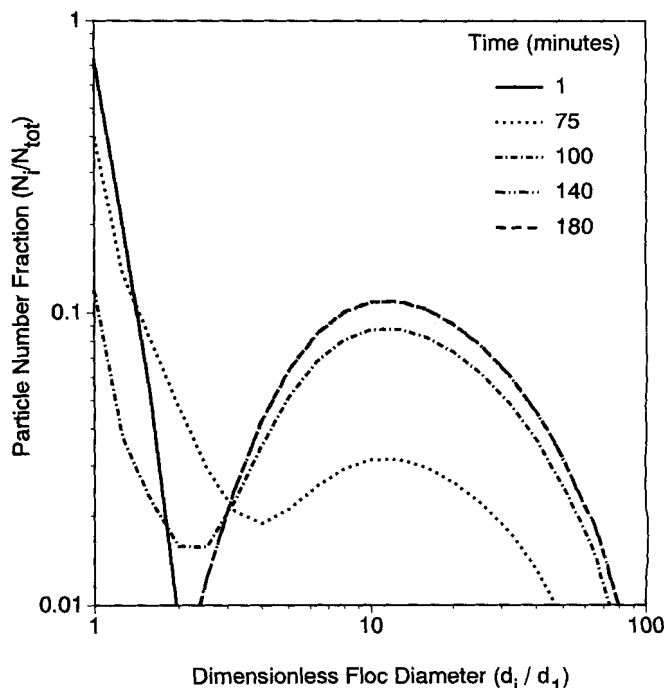


Figure 2. Evolution of the floc-size distribution.

After 140 min, the size distribution has reached steady state.

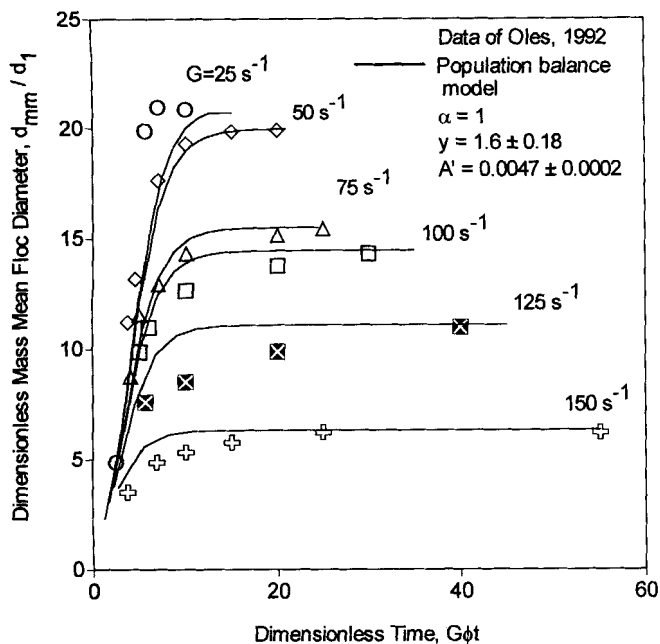


Figure 3. Model predictions vs. experimental data of Oles (1992) for the evolution of the dimensionless mass mean floc diameter.

one needs to consider that model parameters can be obtained from the experimental conditions with the exception of the accommodation coefficient for coagulation α and the fragmentation rate coefficient $A(A', y)$. Values of A and α were determined by matching the evolution of the predicted dimensionless mass mean floc diameter with the experimental data of Oles (1992) for the flocculation of 2.17 μm polystyrene particles with 1 M NaCl at various shear rates, $G = 25\text{--}150\text{ s}^{-1}$ (Figure 3). The parameters A' and y were determined by regression analysis of A as a function of G (Lu and Spielman, 1985).

The model nicely reproduces Oles' data with $\alpha = 1$, $A' = 0.0047 \pm 0.0002$, and $y = 1.6 \pm 0.18$ over the whole G range, especially the asymptotic values of the particle diameter (Figure 3). The first-order behavior exhibited by the model results is also in excellent agreement with the moment analysis of Vigil and Ziff (1989). There is, however, a systematic deviation of the model results from the experimental data with respect to the particle growth rate. At low shear rates (25 s^{-1}), the flocs are more irregular (Thomas, 1964) and may coagulate more rapidly than their spherical mass equivalent counterparts (Wiesner, 1992). The resulting floc growth rates will therefore exceed the theoretical predictions. At higher shear rates ($100\text{--}150\text{ s}^{-1}$), the model overpredicts the floc growth rate because viscous retardation may slow the coagulation rate (Spielman, 1970; Higashitani et al., 1982, 1983; Han and Lawler, 1992). At average shear rates ($50\text{--}75\text{ s}^{-1}$), the enhanced coagulation of the irregular flocs may be compensated for by the viscous effects. Neither of these effects are accounted for by the present model.

The collision efficiency α is related to the degree of electrostatic destabilization of the particles and the hydrodynamic effects they encounter. Various expressions exist relating this parameter to system variables such as ionic strength and viscous retardation of collisions (Saffman and Turner,

1956; Spielman, 1970; Higashitani et al., 1982 and 1983; Han and Lawler, 1992). The $\alpha = 1$ indicates that the suspension was completely destabilized and that all collisions were successful. The complete success of all collisions is unlikely, but the enhanced coagulation induced by the irregularity of the actual flocs may compensate for the reduction of the collision efficiency by viscous effects and increase the observed α .

It is worth noting that Lu and Spielman (1985) also found $y = 1.6$ for flocculation of kaolin with a polymer flocculant at $G = 50\text{--}200\text{ s}^{-1}$. The two parameters y and A' can be related to the strength of the floc, which depends on flocculant type and concentration, surface properties of the primary particles, floc structure, and suspension medium. All of these factors need to be related to the values of y and A' in order to provide an accurate description of the floc breakage kinetics. This work indicates that the simple power law description (Eq. 8) is a useful kinetic model of floc breakage. The agreement between our results and those of Lu and Spielman (1985) for the value of the exponent y offers further reassurance that this type of model is useful in modeling flocculation, considering especially that two completely different particle-flocculant systems were used in the two studies.

Effect of shear on the steady-state floc-size distribution

The steady-state floc-size distribution (Figure 2, $t = 140$ or 180 min) represents the dynamic balance between coagulation and fragmentation. Figure 4a shows the effect of the shear rate G on the steady-state floc-size distribution using the obtained A' and y values from Figure 3. The distributions were considered to be at steady state once their geometric standard deviation σ_g did not change more than 1% (Vemury et al., 1994). For these conditions, increasing G increases the coagulation rate but represents a more pronounced increase in the fragmentation rate, thus shifting the steady-state floc-size distribution into smaller floc sizes (Figure 4a).

When, however, these steady-state floc-size distributions are normalized (scaled) with respect to their arithmetic (number) average floc size d_n and replotted (Swift and Friedlander, 1964; Friedlander and Wang, 1966), they collapse onto a single line, especially the large tail of the distribution (Figure 4b). Hence, the distributions are self-preserving with respect to shear rate. The shape of the steady-state floc-size distribution is not affected by the shear rate once most of the distribution grows well above the primary particle size such as the concentrations of the primary particle size N_1 , which is less than 5% at steady state; $N_{1ss}/N_{tot} < 0.05$; ($G = 10$ or 25 s^{-1}). At higher shear rates ($G = 50$ or 100 s^{-1}), however, when the primary particles constitute a significant fraction of the distribution, though the large tail of the distribution nicely follows the asymptotic one, the small tail does not. Clearly, high shear rates prevent the growth of the size distribution to large enough sizes to exhibit the full self-preserving distribution at steady state. The extent of self-similarity may indicate the stage of development of the steady-state floc-size distribution at a given shear rate.

Polystyrene floc-size distributions at steady state were determined by image analysis (using maximum floc length as floc size) for $G = 63, 95,$ and 129 s^{-1} at an alum concentration of 32 mg/L and $N_0 = 2.5 \times 10^8\text{ cm}^{-3}$ (Spicer, 1995).

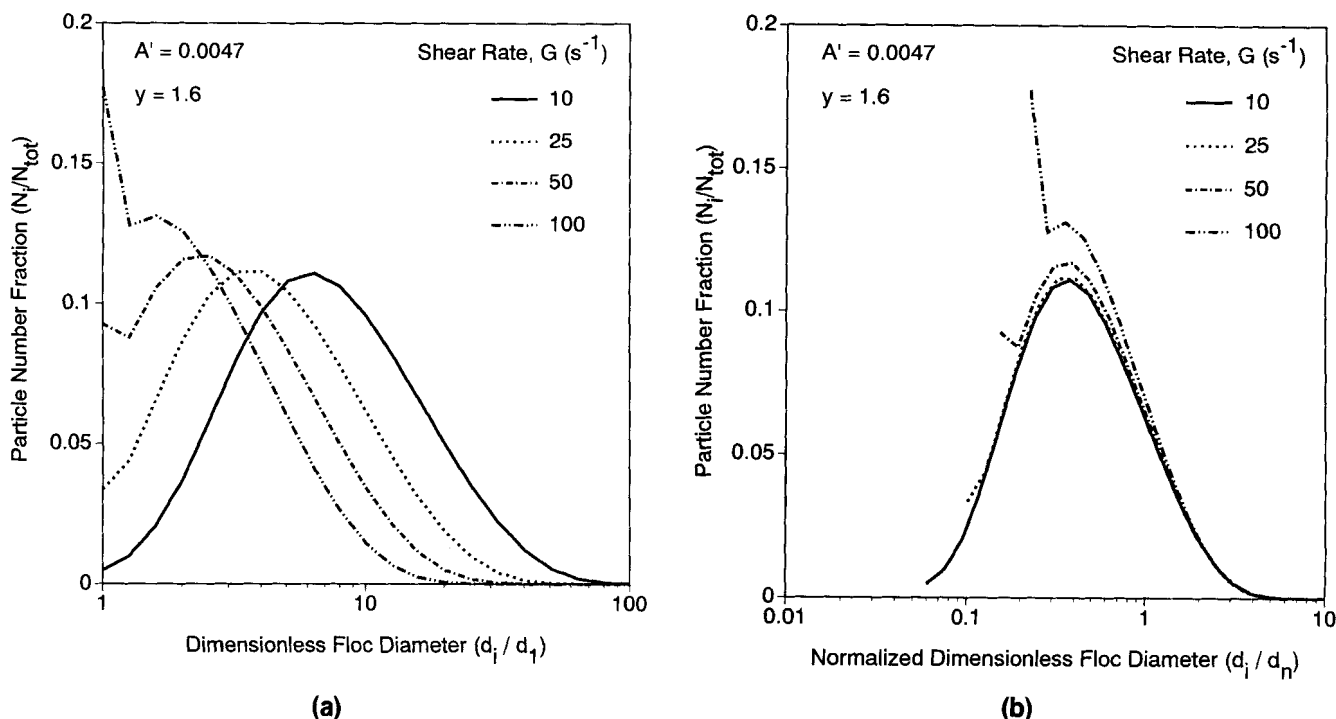


Figure 4. Steady-state floc-size distributions in (a) dimensionless floc-size coordinates (scaled by the diameter of the primary particle size, d_1), (b) normalized for $N_1 = 9.3 \times 10^6 \text{ cm}^{-3}$, $d_1 = 2.17 \text{ }\mu\text{m}$, $\alpha = 1$, $A' = 0.0047$, $\gamma = 1.6$, and various shear rates G .

Increased G results in an increased fragmentation rate and a shift of the floc-size distribution into smaller sizes. Higher G values ($G > 50 \text{ s}^{-1}$) prevent the size distribution from significantly developing beyond the primary particle size. Upon normalization, the distributions collapse onto a single line, especially their large tail.

These distributions are plotted in normalized form in Figure 5 ($L_{63} = 84 \text{ }\mu\text{m}$, $L_{95} = 67 \text{ }\mu\text{m}$, $L_{129} = 42 \text{ }\mu\text{m}$). It is seen that the large tails of these distributions nicely collapse onto each other. The experimental floc-size distributions are completely self-similar, independent of the applied shear rates. This is in agreement with theory, as microscopic experimental observations indicated that no primary particles remained in suspension at steady state. There is some scatter at the lower sizes that is reminiscent of the fragment peaks in Figure 4a, but most likely results from the image analyzer's lower detection threshold. The lower detection threshold of the image analysis software is $5 \text{ }\mu\text{m}$, on the order of the size of the smallest flocs in the size distribution. As a result, there is a larger degree of scatter in the measurements in this size range.

The shape of the theoretical steady-state self-preserving floc-size distribution (Figure 4b) is similar to the experimental one but broader (theoretical $\sigma_{gn} = 2.23$ vs. experimental $\sigma_{gn} \approx 1.7$). A direct comparison between the two distributions is not possible. The model is based on the equivalent volume of primary particles contained in a floc u_i while the image analysis results are based on the maximum floc length L . These two different sizes do not provide a consistent basis for comparison between the model and data. Furthermore, the model does not account for the irregular floc structure, viscous retardation of collisions, and flow field heterogeneity that may very well affect the detailed shape of the self-preserving size distribution with respect to shear. Nevertheless, theory and data clearly show the existence of such a distribution. This distribution is invariant with shear provided that

the operative coagulation and fragmentation rates do not vary over the employed shear range (Spicer and Pratsinis, 1996).

Fragment size distribution and the self-preserving steady-state floc-size distribution

The effect of various types of fragment-size distributions on the self-preserving steady-state size distribution is investigated in Figure 6 for the conditions in Figure 2. A binary fragment size distribution results in the self-preserving size distribution of Figure 4b. The volume- and number-based geometric standard deviations (σ_{gv} and σ_{gn}) of the four distributions in Figure 6 are given in Table 1. The self-preserving steady-state distributions resulting from binary or ternary fragmentation-size distributions are similar though the latter is slightly broader than the former. The increased degree of floc breakage by ternary fragmentation affects the shape of the steady-state floc-size distribution but does not alter its asymptotic behavior. A broad normal ($\lambda = 6$) distribution of fragments makes the self-preserving steady-state distribution even broader. The shapes of the self-preserving size distribution resulting from binary and narrow normal ($\lambda = 10$) distributions are almost identical as a result of the relative breadth of the upper size classes compared to that of the fragment-size distribution. However, when $\lambda = 6$, the steady-state floc-size distribution is broader than at $\lambda = 10$ as a result of the formation of finer particles upon fragmentation (Coulaloglou and Tavlarides, 1977; Alvarez et al., 1994). A broader fragment-size distribution therefore broadens the steady-state

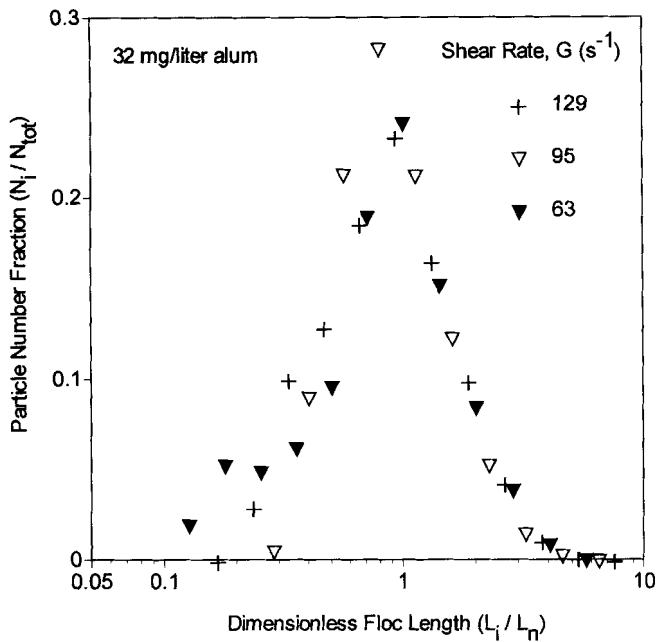


Figure 5. Normalized steady-state floc-size distributions obtained by image analysis of flocs produced at $N_0 = 2.5 \times 10^8 \text{ cm}^{-3}$ as a function of shear rate (63, 95 and 129 s^{-1}) at an alum concentration of 32 mg/L ($L_{63} = 84 \text{ }\mu\text{m}$; $L_{95} = 67 \text{ }\mu\text{m}$; $L_{129} = 42 \text{ }\mu\text{m}$).

The distributions collapse onto each other, indicating that they are self-preserving with respect to shear.

floc-size distribution by increasing the influence of fragmentation on the attainment of steady state.

Conclusions

A model has been presented describing the attainment of a steady-state particle-size distribution by simultaneous coagulation and fragmentation. The model predictions are in qualitative agreement with experimental data of polystyrene-NaCl flocculation in the literature. It is shown that the steady-state floc-size distribution is independent of shear rate when normalized by the average floc size. It is thus self-preserving with respect to shear provided that the coagulation and fragmentation mechanisms do not change in the employed shear range and that no more than 5% (by number) of the initial particles remain unflocculated. The existence of this self-preserving size distribution is supported by our data on alum-polystyrene flocculation. The fragment-size distribution affects the shape of the self-preserving steady-state size distribution. As the fragment-size distribution broadens, so does the self-preserving one.

Acknowledgments

This research was supported by the National Science Foundation, grant CTS-8957042. We acknowledge stimulating discussions with Mr. Srinivas Vemury (Univ. of Cincinnati) during this research and the insightful comments by Professor Jon Olson (Univ. of Delaware) during the review of our manuscript.

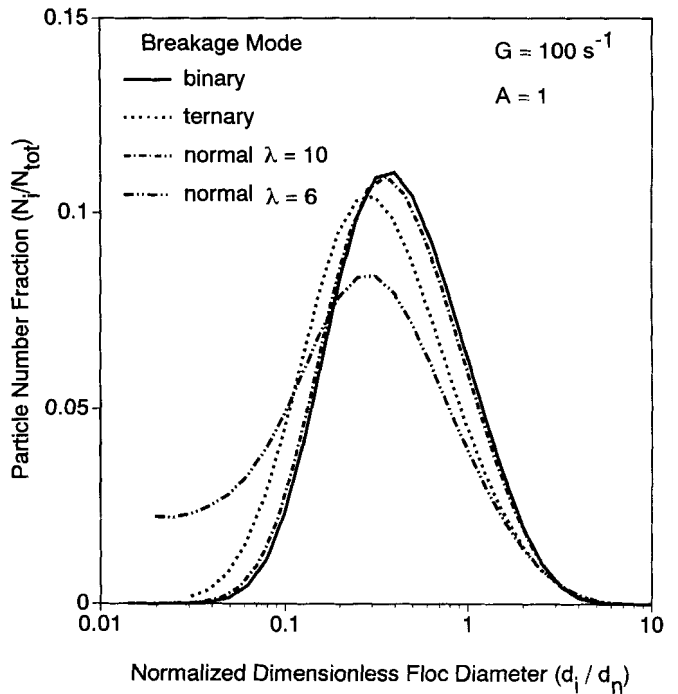


Figure 6. Self-preserving floc-size distributions for simultaneous coagulation and fragmentation of polystyrene particles (base case) resulting from various fragment-size distributions.

A ternary breakage mechanism results in a broader distribution than a binary one as a result of the larger number of fragments produced during a breakage event. A narrow normally distributed fragment size distribution ($\lambda = 10$) gives a self-preserving distribution similar to that of the binary fragment size distribution while a broad ($\lambda = 6$) fragment-size distribution results in a broader self-preserving one.

Notation

- a = power law constant
- A = breakage rate coefficient, $\text{cm}^{-3} \cdot \text{s}^{-1}$
- A' = breakage rate coefficient determining functional dependence of the breakage rate on shear rate, $\text{cm}^{-3} \cdot \text{s}^{-1} \cdot \text{s}^{-a}$
- b_i = upper boundary volume of section i (sectional), cm^3
- d = mass equivalent floc diameter (model results and light-scattering data of Oles (1992)), cm
- d_m = mass mean mass equivalent floc diameter (model results and light-scattering data of Oles (1992)), cm
- d_n = arithmetic (number) mean mass equivalent floc diameter (model results), cm
- d_1 = mass-equivalent diameter of primary particle, cm
- f = sectional spacing factor
- $i \text{ max}$ = index of the largest section
- L_G = arithmetic (number) average maximum floc length at steady state at shear rate G , cm

Table 1. Geometric Standard Deviation of the Steady-State Volume and Number Size Distribution Arising from Simultaneous Coagulation and Fragmentation during Shear-Induced Flocculation

Fragment-Size Distribution	σ_{gv}	σ_{gn}
Binary	1.793	2.232
Ternary	1.948	2.386
Broad Normal Distribution ($\lambda = 6$)	1.906	2.933
Narrow Normal Distribution ($\lambda = 10$)	1.815	2.259

L_n = arithmetic (number) average maximum floc length, cm
 n_i = number concentration of particles of size i (discrete), no./cm³
 N_0 = initial number concentration of primary particles during experiment, no./cm³
 N_i = number concentration of particles in section i (sectional), no./cm³
 N_{iss} = steady-state number concentration of particles in section i (sectional), no./cm³
 N_{tot} = total number concentration of particles (sectional), no./cm³
 S_i = breakage rate, s⁻¹
 t = time, s
 u_i = volume of floc of size i , containing i primary particles (discrete), cm³
 V_{fn} = mean of the fragment size distribution (sectional), cm³
 V_i = volume of characteristic floc of section i , composed of 2^{i-1} primary particles (sectional), cm³

Greek letters

$\beta(V_i, V_j)$ = collision frequency of particles with volume V_i and V_j , cm³/s
 $\Gamma_{i,j}$ = breakage distribution function, volume fraction of i -sized particles produced by breakage of j -sized flocs (sectional)
 ϵ = average turbulent energy dissipation rate, cm³/s²
 λ = factor relating standard deviation of fragment-size distribution to the mean of the distribution
 ν = kinematic viscosity, cm²/s
 σ_f = standard deviation of the fragment-size distribution, cm³
 σ_{gn} = number-based geometric standard deviation
 σ_{gv} = volume-based geometric standard deviation
 ϕ = solids volume fraction of suspended particles, cm³/cm³

Literature Cited

Akers, R. J., A. G. Rushton, and J. I. T. Stenhouse, "Floc Breakage: The Dynamic Response of the Particle Size Distribution in a Flocculated Suspension to a Step Change in Turbulent Energy Dissipation," *Chem. Eng. Sci.*, **42**, 787 (1987).
Alvarez, J., J. Alvarez, and M. Hernandez, "A Population Balance Approach for the Description of Particle Size Distribution in Suspension Polymerization Reactors," *Chem. Eng. Sci.*, **49**, 99 (1994).
Austin, L. G., "A Review: Introduction to the Mathematical Description of Grinding as a Rate Process," *Powd. Tech.*, **5**, 1 (1971).
Blatz, P. J., and A. V. Tobolsky, "Note on the Kinetics of Systems Manifesting Simultaneous Polymerization-Depolymerization Phenomena," *J. Phys. Chem.*, **49**, 77 (1945).
Boadway, J. D., "Dynamics of Growth and Breakage of Alum Floc in Presence of Fluid Shear," *J. Env. Eng. Div.: Proc. ASCE*, **104**, 901 (1978).
Burban, P., W. Lick, and J. Lick, "The Flocculation of Fine-Grained Sediments in Estuarine Waters," *J. Geophys. Res.*, **94**, 8323 (1989).
Camp, T. R., and P. G. Stein, "Velocity Gradients and Internal Work in Fluid Motion," *J. Boston Soc. Civ. Eng.*, **30**, 219 (1943).
Chen, W., R. R. Fisher, and J. C. Berg, "Simulation of Particle Size Distribution in an Aggregation-Breakup Process," *Chem. Eng. Sci.*, **45**, 3003 (1990).
Cohen, R. D., "Steady-State Cluster Size Distribution in Stirred Suspensions," *J. Chem. Soc. Farad. Trans.*, **86**, 2133 (1990).
Cohen, R. D., "Self-Similar Cluster Size Distribution in Random Coagulation and Breakup," *J. Colloid Interf. Sci.*, **149**, 261 (1992).
Coulaloglou, C. A., and L. L. Tavlarides, "Description of Interaction Processes in Agitated Liquid-Liquid Dispersions," *Chem. Eng. Sci.*, **32**, 1289 (1977).
Cutter, L. A., "Flow and Turbulence in a Stirred Tank," *AIChE J.*, **12**, 35 (1966).
Danov, K. D., I. B. Ivanov, T. D. Gurkov, and R. P. Borwankar, "Kinetic Model for the Simultaneous Processes of Flocculation and Coalescence in Emulsion Systems," *J. Colloid Interf. Sci.*, **167**, 8 (1994).
Delichatsios, M. A., and R. F. Probstein, "The Effect of Coalescence on the Average Drop Size in Liquid-Liquid Dispersions," *Ind. Eng. Chem. Fund.*, **15**, 134 (1976).

Family, F., P. Meakin, and J. M. Deutch, "Kinetics of Coagulation with Fragmentation: Scaling Behavior and Fluctuation," *Phys. Rev. Lett.*, **57**, 727 (1986).
Friedlander, S. K., *Smoke, Dust, and Haze*, Wiley, New York (1977).
Friedlander, S. K., and C. S. Wang, "The Self-Preserving Size Distribution for Coagulation by Brownian Motion," *J. Colloid Interf. Sci.*, **22**, 126 (1966).
Godfrey, J. C., F. I. N. Obi, and R. N. Reeve, "Measuring Drop Size in Continuous Liquid-Liquid Mixers," *Chem. Eng. Prog.*, **85**, 61 (1989).
Golovin, A. M., "The Solution of the Coagulation Equation for Raindrops, Taking Condensation into Account," *Bull. Acad. Sci. SSSR Geophys. Ser.*, English translation, 482 (1963).
Grabnerbauer, G. C., and C. E. Glatz, "Protein Precipitation-Analysis of Particle Size Distribution and Kinetics," *Chem. Eng. Comm.*, **12**, 203 (1981).
Han, M., and D. F. Lawler, "The (Relative) Insignificance of G in Flocculation," *J. AWWA*, 79 (1992).
Higashitani, K., K. Yamauchi, Y. Matsuno, and G. Hosokawa, "Kinetic Theory of Shear Coagulation for Particles in a Viscous Fluid," *J. Chem. Eng. Japan*, **15**, 299 (1982).
Higashitani, K., K. Yamauchi, Y. Matsuno, and G. Hosokawa, "Turbulent Coagulation of Particles Dispersed in a Viscous Fluid," *J. Chem. Eng. Japan*, **16**, 299 (1983).
Holland, F. A., and F. S. Chapman, *Liquid Mixing and Processing in Stirred Tanks*, Reinhold, London, Fig. 4-4, p. 78 (1966).
Hounslow, M. J., R. L. Ryall, and V. R. Marshall, "A Discretized Population Balance for Nucleation, Growth, and Aggregation," *AIChE J.*, **34**, 1821 (1988).
IMSL, *User's Manual*, IMSL Math/Library, Vol. 2, Version 1.1, Houston (1989).
Kapur, P. C., "Self-Preserving Size Spectra of Comminuted Particles," *Chem. Eng. Sci.*, **27**, 425 (1972).
Kim, Y. H., and L. A. Glasgow, "Simulation of Aggregate Growth and Breakage in Stirred Tanks," *Ind. Eng. Chem. Res.*, **26**, 1604 (1987).
Konno, M., M. Aoki, and S. Saito, "Scale Effect on Breakup Process in Liquid-Liquid Agitated Tanks," *J. Chem. Eng. Japan*, **16**, 312 (1983).
Kusters, K. A., "The Influence of Turbulence on Aggregation of Small Particles in Agitated Vessels," PhD Thesis, Eindhoven Univ. of Technology, The Netherlands (1991).
Kusters, K. A., S. E. Pratsinis, S. G. Thoma, and D. M. Smith, "Ultrasonic Fragmentation of Agglomerate Powders," *Chem. Eng. Sci.*, **48**, 4119 (1993).
Landgrebe, J. D., and S. E. Pratsinis, "A Discrete-Sectional Model for Particulate Production by Gas-Phase Chemical Reaction and Aerosol Coagulation in the Free-Molecular Regime," *J. Colloid Interf. Sci.*, **139**, 63 (1990).
Lu, C. F., and L. A. Spielman, "Kinetics of Floc Breakage and Aggregation in Agitated Fluid Suspensions," *J. Colloid Interf. Sci.*, **103**, 95 (1985).
Oles, V., "Shear-Induced Aggregation and Breakup of Polystyrene Latex Particles," *J. Colloid Interf. Sci.*, **154**, 351 (1992).
Pandya, J. D., and L. A. Spielman, "Floc Breakage in Agitated Suspensions: Theory and Data Processing Strategy," *J. Colloid Interf. Sci.*, **90**, 517 (1982).
Parker, D. S., W. J. Kaufman, and D. Jenkins, "Floc Breakup in Turbulent Flocculation Processes," *J. San. Eng. Div.: Proc. ASCE*, **98**, 79 (1972).
Peng, S. J., and R. A. Williams, "Direct Measurement of Floc Breakage in Flowing Suspensions," *J. Colloid Interf. Sci.*, **166**, 321 (1994).
Reich, I., and R. D. Vold, "Flocculation-Deflocculation in Agitated Suspensions. I. Carbon and Ferric Oxide in Water," *J. Phys. Chem.*, **63**, 1497 (1959).
Saffman, P., and J. Turner, "On the Collision of Drops in Turbulent Clouds," *J. Fluid Mech.*, **1**, 16 (1956).
Shamlou, P. A., and N. Tichener-Hooker, "Turbulent Aggregation and Breakup of Particles in Liquids in Stirred Vessels," in *Processing of Solid-Liquid Suspensions*, P. A. Shamlou, ed., Butterworth Heinemann, Oxford (1993).
Spicer, P. T., "The Dynamics of Shear-Induced Flocculation in a Stirred Tank," MS Thesis, Univ. of Cincinnati, Cincinnati, OH (1995).
Spicer, P. T., and S. E. Pratsinis, "Shear-Induced Flocculation: The

- Evolution of Floc Structure and the Shape of the Size Distribution at Steady-State," *Water Res.*, **30**, in press (1996).
- Spielman, L. A., "Viscous Interactions in Brownian Coagulation," *J. Colloid Interf. Sci.*, **33**, 562 (1970).
- Sprow, F. B., "Drop Size Distributions in Strongly Coalescing Agitated Liquid-Liquid Systems," *AIChE J.*, **13**, 995 (1967).
- Swift, D. L., and S. K. Friedlander, "The Coagulation of Hydrosols by Brownian Motion and Laminar Shear Flow," *J. Colloid Interf. Sci.*, **19**, 621 (1964).
- Tambo, N., and Y. Watanabe, "Physical Aspect of Flocculation Process: I. Fundamental Treatise," *Water Res.*, **13**, 429 (1979).
- Tambo, N., "Basic Concepts and Innovative Turn of Coagulation/Flocculation," *Water Supply*, **9**, 1 (1991).
- Thomas, D. G., "Turbulent Disruption of Floccs in Small Particle Size Suspensions," *AIChE J.*, **10**, 517 (1964).
- Vemury, S., K. A. Kusters, and S. E. Pratsinis, "Time Lag for Attainment of the Self-Preserving Particle Size Distribution by Coagulation," *J. Colloid Interf. Sci.*, **165**, 53 (1994).
- Vigil, R. D., and R. M. Ziff, "On the Stability of Coagulation-Fragmentation Population Balances," *J. Colloid Interf. Sci.*, **133**, 257 (1989).
- Wiesner, M. R., "Kinetics of Aggregate Formation in Rapid Mix," *Water Res.*, **26**, 379 (1992).
- Williams, M. M. R., "An Exact Solution of the Fragmentation Equation," *Aerosol Sci. Tech.*, **12**, 538 (1990).
- Wright, H., and D. Ramkrishna, "Factors Affecting Coalescence Frequency of Droplets in a Stirred Liquid-Liquid Dispersion," *AIChE J.*, **40**, 767 (1994).

Manuscript received Apr. 24, 1995, and revision received Sept. 11, 1995.